[6] Giesing, J. P., "Nonlinear Two-Dimensional Unsteady Potential Flow with Lift," *Journal of Aircraft*, Vol. 5, No. 2, March–April 1968, pp. 135–143.

[7] Giesing, J. P., "Nonlinear Interaction of Two Lifting Bodies in Arbitrary Unsteady Motion," *Transactions of ASME*, Ser. D; *Journal of Basic Engineering*, Vol. 90, No. 3, Sept. 1968.

[8] Djojodihardjo, R. H. and Widnall, S. E., "A Numerical Method for the Calculation of Nonlinear, Unsteady Lifting Potential Flow Problems," *AIAA Journal*, Vol. 7, No. 10, Oct. 1969.

[9] Milne-Thompson, L. M., *Theoretical Hydrodynamics*, Macmillan Co., New York, 1960.

[10] Giesing, J. P., "Potential Flow About Two-Dimensional Airfoils," LB39146, 1965, Douglas Aircraft Co.

[11] Giesing, J. P., "Two-Dimensional Potential Flow Theory for Multiple Bodies in Small-Amplitude Motion," DAC 67028, April 1968, McDonnell Douglas Aircraft Co.

[12] Giesing, J. P., "Vorticity and Kutta Condition for Unsteady Multi-Energy Flows," *Transactions of ASME*, Ser. E, *Journal of Applied Mechanics*, Vol. 36, No. 3, Sept. 1969.

[13] Sears, W. R., "Some Aspects of Non-Stationary Airofoil Theory and Its Practical Application," *Journal of Aerospace Sciences*, Vol. 8, No. 3, 1941, pp. 104–108.

[14] Giesing, J. P., Rodden, W. P., Stahl, B., "The Sears Function and Lifting Surface Theory for Harmonic Gust Fields," *Journal of Aircraft*, Vol. 7, No. 3 May-June 1970 pp. 252–255.

[15] Drischler, J. A., Diederich, F. W., "Lift and Moment Responses to Penetration of Sharp-Edged Traveling Gusts, with Application to Penetration of Weak Blast Waves," TN 3956, May 1957, NACA.

NOVEMBER 1970 AIAA JOURNAL VOL. 8, NO. 11

Results from a New Wind-Tunnel Apparatus for Studying Coning and Spinning Motions of Bodies of Revolution

LEWIS B. SCHIFF* AND MURRAY TOBAK*
NASA Ames Research Center, Moffett Field, Calif.

An apparatus is described which reproduces either separate or combined coning and spinning motions of a body of revolution in a wind tunnel, using a six-component strain gage balance to measure the aerodynamic forces and moments. Results of experiments with a slender cone in coning motion show that at small angles of attack the side-force and side-moment coefficients normalized by the coning rate are linear functions of the angle of attack, the slopes of which are in excellent agreement with the damping-in-pitch coefficients $C_{N_q} + C_{N_{\dot\alpha}}$ and $C_{m_q} + C_{m_{\dot\alpha}}$. This agreement, predicted by linearized theory, indicates that at small angles of attack the dynamic damping-in-pitch coefficients of a body of revolution can be measured as the steady side force and moment coefficients of the body undergoing coning motion. For larger angles of attack, where vortices appear on the leeside of the body, the normalized side force and moment coefficients become nonlinear functions of angle of attack. Photographs of the vortices reveal that they are displaced from the angle-of-attack plane by coning motion. This asymmetric displacement of the vortices persists over the entire length of the body, making them a possible source of nonlinear side moment.

Nomenclature

A = axial force (Fig. 1)
C_l = rolling-moment coefficient, l/q_0Sl_0
C_m = pitching-moment coefficient, m/q_0Sl_0
C_{m_v} = that contribution to the pitching-moment coefficient attributable to the presence of vortices
C_n = side-moment coefficient, n/q_0Sl_0
$C_{np\alpha}$ = rate of change of linearized side-moment coefficient with respect to p and α; $[\partial^2 C_n/\partial(pl_0/V_0)\partial]_{\alpha\alpha\to 0;\ p\to 0}$ classical Magnus moment coefficient
C_N = normal-force coefficient, N/q_0S
C_{N_v} = that contribution to the normal-force coefficient attributable to the presence of vortices
$C_{N\alpha}, C_{m\alpha}$ = rate of change of linearized normal-force and pitching-moment coefficients with angle of attack; $(\partial C_N/\partial\alpha)_{\alpha\to 0}$, $(\partial C_m/\partial\alpha)_{\alpha\to 0}$
C_{N_q}, C_{m_q} = rate of change of linearized normal-force and pitching-moment coefficients with pitching velocity parameter ql_0/V_0; $[\partial C_N/\partial(ql_0/V_0)]_{q\to 0}$, $[\partial C_m/\partial(ql_0/V_0)]_{q\to 0}$
$C_{N\dot\alpha}, C_{m\dot\alpha}$ = rate of change of linearized normal force and pitching-moment coefficients with time rate of change of angle-of-attack parameter $\dot\alpha l_0/V_0$ $[\partial C_N/\partial(\dot\alpha l_0/V_0)]_{\dot\alpha\to 0}, [\partial C_m/\partial(\dot\alpha l_0/V_0)]_{\dot\alpha\to 0}$
$C_m\{\infty;\sigma(t),0,0\}$ = pitching-moment coefficient in steady planar motion with σ held fixed at $\sigma(t)$; zeroes denote ϕ and ψ respectively held fixed at zero
$C_{m_{\dot\alpha}}\{\sigma(t),0,0\}$ = damping-in-pitch coefficient in planar motion (ϕ and ψ held fixed at zero) measured about a fixed inclination σ = const
$C_{n\dot\phi}\{\infty;\sigma(t),0,0\}$ = rate of change with respect to coning rate parameter $\dot\phi l_0/V_0$ of the side-moment coefficient measured in steady coning motion (with σ held fixed at $\sigma(t)$, ϕ held fixed at a series of values, and ψ held fixed at zero), evaluated at $\dot\phi = 0$
$C_{n\dot\psi}\{\infty;\sigma(t),0,0\}$ = rate of change with respect to spin rate parameter $\dot\psi l_0/V_0$ of the side-moment coefficient measured in steady spinning motion (with σ held fixed at $\sigma(t)$, ψ held fixed at a series of values, and ϕ held fixed at zero), evaluated at $\dot\psi = 0$
C_Y = side-force coefficient, Y/q_0S
l_{cg} = length along body axis of symmetry from nose to center of rotation (Fig. 2)

Received February 20, 1970; revision received May 11, 1970.
* Research Scientist. Member AIAA.

l_0 = characteristic length (body length in experiment)
l = rolling moment (Fig. 1)
M_0 = freestream Mach number
m = pitching-moment (Fig. 1)
n = side moment (Fig. 1)
N = normal force (Fig. 1)
p = component of angular velocity about body x axis; $p = \dot{\psi} + \dot{\phi}\cos\sigma$
q_0 = dynamic pressure, $(\frac{1}{2})\rho_0 V_0^2$
Re = freestream unit Reynolds number $\rho_0 V_0/\mu$
S = characteristic area (body base area in experiment)
t = time
V_0 = freestream velocity
X_e, Y_e, Z_e = orthogonal axes having fixed directions in space, origin at the center of rotation (Fig. 1)
x, y, z = orthogonal axes fixed in the body, origin at the center of rotation (Fig. 1)
Y = side force (Fig. 1)
γ = angle between the plane of the resultant angle of attack and the plane of symmetry of the vortices, measured at a given value of x in a plane normal to the x axis
μ = freestream viscosity
ρ_0 = freestream density
ϕ, σ, ψ = Eulerian angles with σ measuring the resultant angle of attack (Fig. 1)
(∞) = denotes steady flow conditions
$(\dot{})$ = $d/dt(\ )$

Introduction

In a previous study[1] a nonlinear formulation of the aerodynamic moment system was presented, which showed that the presence of coupling for a body undergoing nonplanar motions is characterized by the moments acting on the body in coning motion. By coupling we mean the following: Consider a nonplanar motion with sufficiently small spin so that the classical Magnus terms are negligible. The motion is equivalently the vector sum of two planar motions. Within a linear formulation of the moment system, the superposition principle justifies treating each planar motion in the absence of the other. The more general formulation shows that the moments caused by motion in one plane are influenced by the presence of the other motion, and this influence is what is meant by coupling. Also presented in Ref. 1 were the results of experiments with a simple device designed to reproduce coning motion of a body of revolution in a wind tunnel, which indicated that the leeside vortices may play a major role in coupling. The apparatus permitted only measurements of the aerodynamic moments due to loads acting forward of the center of rotation, and visualization of the vortices was likewise limited to the part of the body ahead of the center of rotation. In order to study the behavior of the vortices over the entire length of the body, and to obtain complete force and moment data, a more sophisticated apparatus utilizing a six-component strain gage balance was constructed. The present paper describes the capabilities and features of the new apparatus. Results of experiments with a slender cone model in coning motion are presented which attempt to relate coupling to the effects of the leeside vortices. The results of concurrent vapor screen studies are used in an attempt to explain the coupling.

With lateral motion of the center of gravity eliminated by condition 1 below, the motion is equivalent to that of a body rotating about a fixed point in a wind tunnel. This makes it convenient to use the gyroscopic coordinate system illustrated in Fig. 1 to describe the motion. Orthogonal axes X_e, Y_e, Z_e are reference axes having fixed orientation and location in space, with origin at the center of rotation. The X_e, Y_e, Z_e axes correspond to axes fixed in the wind tunnel. The oncoming flow, having velocity V_0, is in the negative X_e direction. Orthogonal axes x, y, z are body-fixed axes with origin at the center of rotation. The x axis is chosen as the axis of cylindrical symmetry. The orientation of the body-fixed axes relative to the X_e, Y_e, Z_e axes is specified by the Euler angles ϕ, σ, ψ with σ measuring the resultant angle of attack. Because the body has cylindrical symmetry, it is convenient to define the aerodynamic forces and moments relative to the σ plane. Thus m, the pitching moment, is the moment about an axis normal to the σ plane; n, the side moment, is the moment about an axis in the σ plane and normal to the x axis. The rolling moment l is the moment about the x-axis. The axial force A is the force in the negative x direction; N, the normal force, is the force in the σ plane and normal to the x axis; Y, the side force, is the force normal to the σ plane.

Analysis

Coordinate System

The nonlinear aerodynamic moment system for bodies undergoing nonplanar motions[1] is subject to the following restrictions: 1) The body's center of gravity traverses a straight path at constant velocity. 2) Atmospheric density is constant along the flight path. 3) The body has cylindrical symmetry about the longitudinal axis.

Nonlinear Formulation

The nonlinear formulation of the aerodynamic moment system for a body possessing cylindrical symmetry and traversing a straight path is [1]

$$C_m(t) = C_m\{\infty;\sigma(t),0,0\} + (\dot{\sigma}l_0/V_0)C_{m\dot{\sigma}}\{\sigma(t),0,0\} \quad (1a)$$

$$C_n(t) = (\dot{\varphi}l_0/V_0)C_{n\dot{\varphi}}\{\infty;\sigma(t),0,0\} + (\dot{\psi}l_0/V_0)C_{n\dot{\psi}}\{\infty;\sigma(t),0,0\} \quad (1b)$$

$$C_l(t) = 0 \quad (1c)$$

The corresponding equations for $C_N(t)$ and $C_Y(t)$ are obtained by replacing m by N and n by Y where they appear in the aforementioned equations. Because of the assumed linear dependence on angular rates the formulation is valid only for low reduced frequencies, but the dependence on angle-of-attack σ is arbitrary. Each coefficient in Eq. (1) has a definite physical meaning, and may be measured individually by the performance of an appropriate experiment. In the expression for the pitching moment coefficient $C_m(t)$, the first coefficient is the pitching-moment coefficient that would be measured with the model attitude held fixed at the instantaneous angle-of-attack $\sigma(t)$. The second coefficient is the planar damping-in-pitch coefficient evaluated from small oscillations in σ about a mean angle of attack equal to the instantaneous angle-of-attack $\sigma(t)$. In the expression for the side-moment coefficient $C_n(t)$, the first coefficient is the rate of change with $\dot{\phi}l_0/V_0$, evaluated at $\dot{\phi} = 0$, of the side-moment coefficient that would be measured in a steady coning motion $\sigma = \text{const}$, $\dot{\phi} = \text{const}$, $\dot{\psi} = 0$. The second coefficient is the rate of change with $\dot{\psi}l_0/V_0$, evaluated at $\dot{\psi} = 0$, of the side-moment coefficient that would be measured in the classical Magnus experiment $\sigma = \text{const}$, $\dot{\psi} = \text{const}$, $\dot{\phi} = 0$.

For small σ, where a linearized theory can be expected to hold, considerations of symmetry require that certain combinations of coefficients in Eq. (1) be equal. For larger σ, however, there are no such necessary connections between any of the coefficients. Thus, Eq. (1) suggests that the moment system for arbitrary σ may be compounded of the contributions from four separate motions. The experimental apparatus to be described subsequently can perform three of the motions and thereby enables the measurement of three of the contributions: $C_m\{\infty;\sigma(t),0,0\}$, $C_{n\dot{\phi}}\{\infty;\sigma(t),0,0\}$ and $C_{n\dot{\psi}}\{\infty;\sigma(t),0,0\}$.

Linear Formulation

The linear formulation of the aerodynamic moment system, valid for low reduced frequencies and to first order in σ, is

$$C_m(t) = \sigma C_{m\alpha}(\infty) + (\dot{\sigma}l_0/V_0)(C_{mq}(\infty) + C_{m\dot{\alpha}}) \quad (2a)$$

$$C_n(t) = \sigma(\dot{\phi}l_0/V_0)(C_{m_q}(\infty) + C_{m\dot{\alpha}}) + \sigma(\dot{\phi} + \dot{\psi})l_0/V_0 C_{np\alpha}(\infty) \quad (2b)$$

$$C_l(t) = 0 \quad (2c)$$

Here, the coefficients are constants. For negligible Magnus moment coefficient $C_{np\alpha}$, the absence of coupling in the linear formulation is reflected in Eq. (2) by the presence of $C_{m_q} + C_{m\dot{\alpha}}$ in both the side-moment and pitching-moment expressions.

By direct comparison with Eq. (1), we have the following equalities, valid, it should be emphasized, only to first order in σ:

$$\sigma C_{m\alpha}(\infty) = C_m\{\infty;\sigma(t),0,0\} \quad (3a)$$

$$C_{m_q}(\infty) + C_{m\dot{\alpha}} = C_{m\dot{\sigma}}\{(\sigma(t),0,0)\} \quad (3b)$$

$$\sigma(C_{m_q}(\infty) + C_{m\dot{\alpha}} + C_{np\alpha}(\infty)) = C_{n\dot{\varphi}}\{\infty;\sigma(t),0,0\} \quad (3c)$$

$$\sigma C_{np\alpha}(\infty) = C_{n\dot{\psi}}\{\infty;\sigma(t),0,0\} \quad (3d)$$

Thus, within a linear theory, Eq. (3) indicates that

$$C_{m_q}(\infty) + C_{m\dot{\alpha}} = (1/\sigma)(C_{n\dot{\varphi}} - C_{n\dot{\psi}}) \quad (4)$$

This result suggests that the linear damping-in-pitch coefficient, a dynamic quantity, may be obtainable from steady measurements of the side-moment contributions caused by separate coning and spinning motions. Since the experimental apparatus enables the individual measurements of $C_{n\dot{\varphi}}$ and $C_{n\dot{\psi}}$ to be carried out, it will be possible to determine whether the suggestion is true.

Experiment

Test Objectives

Results of previous experiments with a simple apparatus that reproduced the coning motion of an ogive-cylinder model in a wind tunnel[1] indicated significant coupling effects caused primarily by asymmetric vortex displacement relative to the angle-of-attack plane. To more fully study the coupling, a new, more sophisticated, apparatus was constructed to reproduce either separate or combined coning (σ = const, $\dot{\phi}$ = const, $\dot{\psi} = 0$) or spinning (σ = const, $\dot{\phi} = 0$, $\dot{\psi}$ = const) motions in a wind tunnel. The coefficients $C_m\{\infty;\sigma(t),0,0\}$, $C_{n\dot{\phi}}\{\infty:\sigma(t),0,0\}$ and $C_{n\dot{\psi}}\{\infty;\sigma(t)0,0\}$ can be measured with the new apparatus.

The apparatus was used to conduct tests of a 10° half-angle cone model in a supersonic wind tunnel. The tests had the following two objectives: 1) at low angles of attack, to determine whether the indication of the linear formulation of the aerodynamic moment system holds; that is, whether the damping-in-pitch coefficients can be obtained from the steady side-force and side-moment measurements and 2) at higher angles of attack, to investigate the behavior of the leeside vortices, and their effects on coupling.

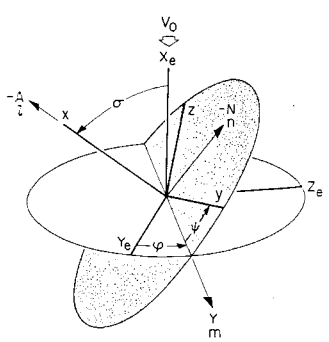

Fig. 1 Coordinate system and moment coefficients.

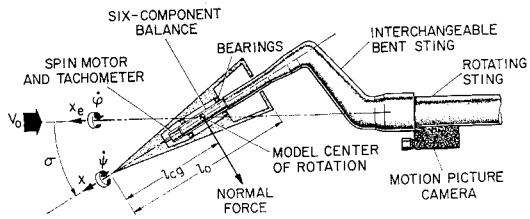

Fig. 2 Apparatus for coning and spinning motion experiment.

Apparatus and Tests

A scale drawing of the apparatus used to reproduce coning and spinning motions in a wind tunnel is presented in Fig. 2. A six-component strain gage balance was fixed rigidly to the sting at the resultant angle of attack σ. The angle of attack could be fixed at various values between 0° and 30° by means of interchangeable bent stings. The bent stings were constructed so that the same axial station of the model remained on the axis of rotation of the sting (that is, the X_e axis) at all angles of attack. This station, the model center of rotation, (also referred to as the model moment center) coincides with the origin of the coordinate system. Measured moments were transferred to a moment center located at this point.

The balance normal force gages were alined with the resultant angle-of-attack plane so that both N, the normal force, and m, the pitching moment, could be determined from steady measurements made by the normal force gages. Similarly, Y, the side force, and n, the side moment, were determined from steady measurements made by the side force gages. Finally, l, the rolling moment, and A, the axial force, were obtained from steady measurements made by the roll and axial gages, respectively. A hydraulic drive motor rotated the sting through a range of speeds from −600 to +600 rpm to reproduce the coning rate $\dot{\phi}$. The model, a 10° half-angle cone 22.8-in. long, was mounted in bearings on the balance. An electric spin motor located in front of the balance rotated the model about the balance axis (i.e., x axis) through a range of speeds from −600 to +600 rpm to reproduce the spin rate $\dot{\psi}$. The balance and tachometer output signals passed through slip rings at the rear of the rotating sting and were connected to the data recording system. Centrifugal and gyroscopic forces caused by the rotation of the apparatus were accounted for by tare measurements.

Because the earlier experiments indicated that the vortices on the leeside of the body may be a potent source of coupling, provision was made to investigate their behavior. The vortices were made visible by the vapor screen technique.[2] A plane of light, or light screen, was passed across the test section normal to the flow velocity. The position of the light screen could be varied at will from the nose to the rear of the model. Water introduced into the test section produced a fog that was illuminated in a single plane by the light screen. The leeside vortices, which appeared in the light screen as dark blobs, were photographed by a motion picture camera mounted rigidly to the rotating sting. Since both the vortex patterns and the camera rotated with the model, the pattern seen by the camera remained essentially steady with time.

Tests with the apparatus were conducted in the Ames 6- × 6-Foot Wind Tunnel at Mach numbers of 1.4 and 2, and at freestream unit Reynolds numbers from 1.5×10^6 to 3.5×10^6/ft.

Results of Balance Measurements

No significant effect of Reynolds number on the forces and moments was observed over the Reynolds number range covered in the test, 1.5×10^6 to 3.5×10^6 per ft. Therefore, the data for the various Reynolds numbers were averaged in the following results.

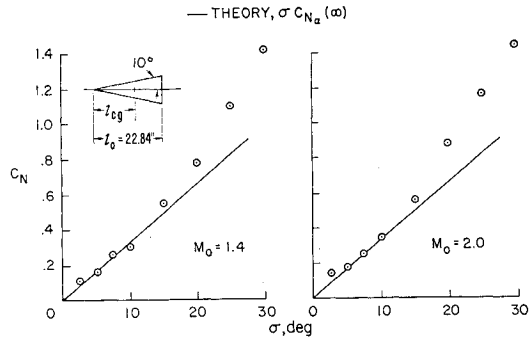

Fig. 3 Normal force coefficients for 10° half-angle cone; $l_{cg}/l_0 = 0.61$, $\dot{\psi} = 0$.

1) Measurements for $C_{Y\dot{\psi}}$ and $C_{n\dot{\psi}}$. The classical Magnus experiment (σ = const, $\dot{\psi}$ = const, $\dot{\phi} = 0$) was carried out over the range of σ from 0° to 30° and for spin rates $\dot{\psi}$ ranging from −600 to +600 rpm. In no case were measurable values of $C_{Y\dot{\psi}}$ or $C_{n\dot{\psi}}$ recorded. In addition, an experiment with combined coning and spinning motions was carried out for the aforementioned range of σ. With $\dot{\phi}$ held fixed at 600 rpm, $\dot{\psi}$ was varied from −600 to +600 rpm. No measurable changes in the side force or side moment were observed as $\dot{\psi}$ was varied. It is concluded that at least over the range of variables covered, $C_{Y\dot{\psi}}$ and $C_{n\dot{\psi}}$ are essentially zero for the 10° half-angle cone. This in effect confirms Sedney's theoretical prediction (cf. Ref. 3). The coefficients would be expected to become substantial for bodies of higher fineness ratio (cf. Ref. 4, Figs. 7–17).

2) Measurements for normal-force and pitching-moment coefficients. Normal-force and pitching-moment coefficients are presented in Figs. 3 and 4, respectively. These coefficients were obtained from data taken with the model coning at various coning rates. At fixed angle of attack, no changes in the normal-force or pitching-moment coefficients were observed due to the coning motion. This confirms that, at least over the range of angle of attack covered in the test (0°–30°), contributions to C_N and C_m due to $\dot{\phi}$, omitted in the nonlinear formulation, Eq. (1), are indeed negligible.

Also shown on Figs. 3 and 4 are the theoretical values[5] of the linear normal-force and pitching-moment coefficients $\sigma C_{N\alpha}(\infty)$ and $\sigma C_{m\alpha}(\infty)$, respectively. At low angles of attack there is good agreement between experimental and theoretical values. The scatter of the data occurs because the centrifugal tare loads caused by coning motion are of the same order as the aerodynamic loads. (The centrifugal tare loads affect only the normal force and pitching moment. Since the side force and side moment are not affected, less scatter is observed in the latter measurements.) At angles of attack greater than the cone half angle, vortices are observed on the leeside of the cone. Under these conditions, the normal-force and pitching-moment coefficients become nonlinear functions of σ, and both are greater than those predicted by the linear theory.

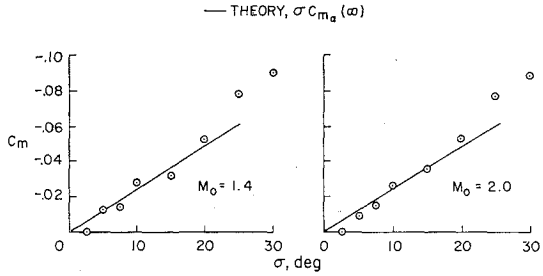

Fig. 4 Pitching-moment coefficients for 10° half-angle cone; $l_{cg}/l_0 = 0.61$, $\dot{\psi} = 0$.

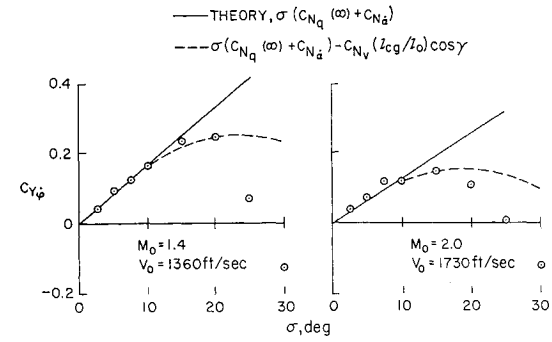

Fig. 5 Side-force coefficient on 10° half-angle cone caused by coning motion; $l_{cg}/l_0 = 0.61$, $\dot{\psi} = 0$.

3) Measurements for $C_{Y\dot{\phi}}$ and $C_{n\dot{\phi}}$. The coning experiment (σ = const, $\dot{\phi}$ = const, $\dot{\psi} = 0$) was carried out over the range of σ from 0° to 30° and for coning rates $\dot{\phi}$ ranging from −600 to +600 rpm. At fixed angle of attack, C_Y and C_n were found to be linear functions of the coning rate over the range of $\dot{\phi}$ investigated. The adequacy of the nonlinear formulation [Eq. (1)], in which only terms linear in $\dot{\phi}$ are retained, is confirmed in this respect.

With linearity in $\dot{\phi}$ confirmed, normalizing C_Y and C_n by the coning-rate parameter $\dot{\phi}l_0/V_0$ gives $C_{Y\dot{\phi}}$ and $C_{n\dot{\phi}}$. Results for these coefficients are presented in Figs. 5 and 6. At low angles of attack, $C_{Y\dot{\phi}}$ and $C_{n\dot{\phi}}$ are seen to be linear functions of σ. Also shown in Figs. 5 and 6 are the theoretical values[5] of the damping-in-pitch parameters $\sigma(C_{N_q}(\infty) + C_{N\dot{\alpha}})$ and $\sigma(C_{m_q}(\infty) + C_{m\dot{\alpha}})$, respectively. There is clearly excellent agreement between the theoretical and experimentally obtained values for angles of attack up to the cone half angle. Since $C_{Y\dot{\psi}}$ and $C_{n\dot{\psi}}$ were found to be negligibly small, this tends to confirm that the predictions by the linear theory [Eq. (4)] of equalities between $\sigma(C_{N_q}(\infty) + C_{N\dot{\alpha}})$ and $(C_{Y\dot{\phi}} - C_{Y\dot{\psi}})$ and between $\sigma(C_{m_q}(\infty) + C_{m\dot{\alpha}})$ and $(C_{n\dot{\phi}} - C_{n\dot{\psi}})$ indeed hold over the range of σ where $C_{Y\dot{\phi}}$ and $C_{n\dot{\phi}}$ vary linearly with σ. It follows that the linear damping-in-pitch parameters are in fact obtainable from steady measurements of the side-force and moment contributions caused by separate coning and spinning motions.

It is recognized that the aforementioned confirmation of the equalities predicted within a linear analysis would have been even more convincingly demonstrated had the experimental results for $C_{Y\dot{\phi}}$ and $C_{n\dot{\phi}}$ been compared and shown to agree with experimental rather than theoretical values of the damping-in-pitch parameters. Experimental values of the damping-in-pitch parameters for the conditions of the present test were not available. Numerous experiments under similar conditions, however, (cf., in particular, Ref. 6) have shown that the theory of Ref. 5 does in fact reliably predict the damping-in-pitch in the low supersonic Mach number range covered in the present test.

At angles of attack greater than the cone half angle, $C_{Y\dot{\phi}}$ and $C_{n\dot{\phi}}$ become nonlinear functions of σ. This nonlinearity is attributed to the appearance and asymmetric displacement of the leeside vortices. Although a conclusive demonstration will require a separate experiment for $C_{m\dot{\alpha}}$, it is considered almost certain that the equality shown to hold at small σ between $\sigma(C_{m_q} + C_{m\dot{\alpha}})$ and $C_{n\dot{\phi}}$ will not hold at larger σ where the coefficients become nonlinear functions of σ. Theoretical considerations suggest that the appearance of vortices should have a relatively small effect on $C_{m\dot{\alpha}}$ (effects on $C_{m\dot{\alpha}}$ and C_{m_q} should tend to compensate), whereas, as can be seen in Fig. 6, $C_{n\dot{\phi}}$ peaks and then tends toward destabilizing values.

Results of Visual Studies of Coning Motion

Sketches typical of the vortex patterns seen in the vapor screen during coning motion are presented in Fig. 7. These represent the patterns above the cone as seen in a crossflow

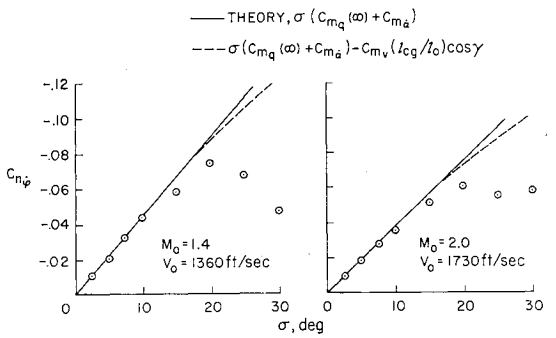

Fig. 6 Side-moment coefficient on 10° half-angle cone caused by coning motion; $l_{cg}/l_0 = 0.61$, $\dot\psi = 0$.

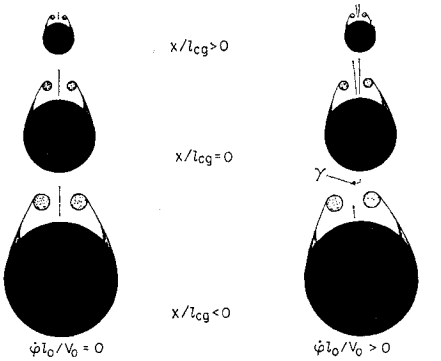

Fig. 7 Schematic representation of vortex displacement during coning motion.

plane (i.e., a plane perpendicular to the body axis of cylindrical symmetry) for angles of attack greater than the cone half angle. At each of three axial stations, one forward of the center of rotation, one at the center of rotation, and one aft of the center of rotation, representative results for zero and positive values of the coning-rate parameter $\dot\phi l_0/V_0$ are shown. The angle-of-attack plane (i.e., the plane containing σ) is vertical in all sketches. For the crossflow plane located forward of the center of rotation, coning motion shifts the axis of symmetry of the vortices from the angle-of-attack plane by an angle γ, the shift being in the direction of the wind in the crossflow plane. The magnitude of γ is approximately that of the angle of the relative wind in a crossflow plane near the nose, that is, $\tan\gamma \approx \dot\phi l_{cg}/V_0$. For clarity, γ is shown approximately three times as large as the maximum observed (about 2°). For a given coning rate, γ appears to have essentially the same value at all stations along the cone, even though at the center of rotation the relative wind is in the angle-of-attack plane, and behind the center of rotation the relative wind is in the direction of negative γ. This result tends to strengthen the suggestion[1] that the displacement of the vortices is not strongly dependent on local flow conditions, but rather is determined principally by flow conditions at the point of the origin of the vortices.

An attempt similar to that described in Ref. 1 was made to link the behavior of the vortices in coning motion with the nonlinear behavior of the side force and moment coefficients $C_{Y\dot\phi}$ and $C_{n\dot\phi}$. From the measurements of the normal force coefficient, an estimate was made of C_{N_v}, the contribution to the normal-force coefficient attributable to the presence of vortices. This contribution was assumed to be the difference between the measured value of $C_N\{\infty;\sigma(t),0,0\}$ and the value given by linearized theory $\sigma C_{N\alpha}(\infty)$. As suggested by the results of the vapor-screen studies, it was assumed that the main effect of coning was to shift the vortices, otherwise unchanged, by the constant angle γ, where γ was given by $\tan^{-1}(\dot\varphi l_{cg}/V_0)$. Under this assumption, multiplying C_{N_v} by $\sin\gamma$ gave an estimate of the side force caused by the shifted vortices. Dividing by $\dot\phi l_0/V_0$ to form the coefficient $C_Y/(\dot\phi l_0/V_0)$ gave $-C_{N_v}(l_{cg}/l_0)\cos\gamma$. This was added to the theoretical linear value of the side force coefficient to yield $C_{Y\dot\phi} = \sigma(C_{N_q}(\infty) + C_{N\dot\alpha}) - C_{N_v}(l_{cg}/l_0)\cos\gamma$. The result is shown plotted on Fig. 5. Carrying out a similar calculation with C_{m_v}, the contribution to pitching-moment coefficient attributable to the presence of vortices gave $C_{n\dot\phi} = \sigma(C_{m_q}(\infty) + C_{m\dot\alpha}) - C_{m_v}(l_{cg}/l_0)\cos\gamma$, shown plotted on Fig. 6. The curves are seen to follow the general trend of the experimental results, but fail to account for the full measure of nonlinearities observed. A more precise description of the vortices in coning motion would appear to be required, in which the vortices are allowed to be of unequal strength. Nevertheless, it seems probable that the observed nonlinearities in $C_{Y\dot\phi}$ and $C_{n\dot\phi}$ can be attributed to the presence and asymmetric disposition of the leeside vortices.

Concluding Remarks

An apparatus which can reproduce either separate or combined coning and spinning motions of a body of revolution in a wind tunnel was described. Results of experiments with a slender cone in coning motion showed that at low angles of attack the side-force and side-moment coefficients normalized by the coning rate are linear functions of the angle of attack. The slopes of these functions are in excellent agreement with theoretical values of the damping-in-pitch coefficients. This result demonstrated that the linearized formulation does describe the aerodynamic forces and moments for bodies of revolution in nonplanar motion whose resultant angle of attack is below that needed for the development of well-defined leeside vortices. Further, it indicated the ability to determine the dynamic damping-in-pitch coefficients of a body of revolution at small angles of attack from the steady side-force and side-moment coefficients measured for the body undergoing steady coning motion. For larger angles of attack, however, where vortices are observed on the leeside of the body, the experimental results showed that the normalized side-force and side-moment coefficients become nonlinear functions of the angle of attack, and tend to become destabilizing. Photographs of the vortices showed that they are displaced from the angle of attack plane by coning, and remain shifted over the entire length of the cone. This result was used in an attempt to explain the nonlinear behavior of the side force and side moment.

References

[1] Tobak, M., Schiff, L. B., and Peterson, V. L., "Aerodynamics of Bodies of Revolution in Coning Motion," *AIAA Journal*, Vol. 7, No. 1, Jan. 1969, pp. 95–99.

[2] Allen, H. J. and Perkins, E. W., "A Study of Effects of Viscosity on Flow Over Slender Inclined Bodies of Revolution," Rept. 1048, 1951, NACA.

[3] Sedney, R., "Laminar Boundary Layer on a Spinning Cone at Small Angles of Attack in a Supersonic Flow," *Journal of the Aeronautical Sciences*, Vol. 24, No. 6, June 1957, pp. 430–436.

[4] Murphy, C. H., "Free Flight Motion of Symmetric Missiles," Rept. 1216, July 1963, Ballistic Research Lab., Aberdeen Proving Ground, Md.

[5] Tobak, M. and Wehrend, W. R., "Stability Derivatives of Cones at Supersonic Speeds," TN 3788, 1956, NACA.

[6] Jaffe, P. and Prislin, R. H., "Effect of Boundary-Layer Transition on Dynamic Stability," *Journal of Spacecraft and Rockets*, Vol. 3, No. 1, Jan. 1966, pp. 46–52.